Optical and electronic properties of bismuth-implanted glasses

M. A. Hughes,[a] Y. Federenko,[a] T. H. Lee,[c] J. Yao,[b] B. Gholipour,[b] R. M. Gwilliam,[a] K. P. Homewood,[a] D. W. Hewak,[b] S. R. Elliott,[c] and R. J. Curry[a]

[a]Advanced Technology Institute, Department of Electronic Engineering, University of Surrey, Guildford, GU2 7XH, United Kingdom; [b]Optoelectronics Research Centre, University of Southampton, Southampton SO17 1BJ, United Kingdom; [c]Department of Chemistry, University of Cambridge, Lensfield Road, Cambridge, CB2 1EW, United Kingdom

Abstract

Photoluminescence (PL) and excitation spectra of Bi melt doped oxide and chalcogenide glasses are very similar, indicating the same Bi center is present. When implanted with Bi, chalcogenide, phosphate and silica glass, and BaF_2 crystal all display characteristically different PL spectra to when Bi is incorporated by melt-doping. This indicates that ion implantation is able to generate Bi centers which are not present in samples whose dopants are introduced during melting. Bi-related PL bands have been observed in glasses with very similar compositions to those in which carrier-type reversal has been observed, indicating that these phenomena are related to the same Bi centers, which we suggest are interstitial Bi^{2+} and Bi clusters.

Keywords: bismuth, implantation, chalcogenide, photoluminescence

*Electronic mail: m.a.hughes@surrey.ac.uk

1. Introduction

Bismuth-doped glasses can give rise to photoluminescence (PL) at wavelengths ranging from 400 nm [1] to 2500 nm [2], under variation of the pump wavelength and composition of the host glass. A wide variety of traditional glass hosts containing Bi have been investigated to date, mainly silicates [3-5] and germanates [6-8], but also phosphates [9], borates [10], chalcogenides [11, 12] and chlorides [2]. The origin of the infrared emission from Bi-doped glasses remains controversial, with convincing arguments being made for a variety of different emission centers, including Bi^{+} [10], Bi^{5+} [13, 14], Bi metal clusters [8], point defects [15] and negatively charged Bi_2 dimers [16, 17]. However, there is a general consensus developing that more than one Bi center is responsible for the observed optical activity of the Bi dopant in glass. Pb doping has also been shown to have very similar absorption and PL behavior to that of Bi in glasses [15]. Broadband Bi-doped fiber lasers operating at wavelengths between 1150 and 1550 nm [18], with powers up to 20 W [19] and slope efficiencies of up to 30% [20], have been reported. A mode-locked Bi-doped fiber laser with 900 fs pulses has also been demonstrated [21]. Bismuth-doped glasses are therefore, potentially, an extremely important class of material for use in broadband lasers and optical amplifiers. One of the main limitations of Bi-doped fiber lasers fabricated so far is the inability to obtain lasing with doping concentrations more than around 0.005 wt% [22]. This means that the fibers need to be on the order of 100 m in length, which causes problems of background loss and nonlinearities. Absorption tails located close to lasing wavelengths cause additional losses [23]. The presence of Bi centers not involved in the lasing process could cause concentration quenching and absorption losses. Therefore, an understanding of the nature of the Bi centers, and the ability to control which Bi centers are present, is critical for the ability to increase doping concentration, reduce losses and bring the performance of Bi-doped fiber lasers in line with that of rare-earth-doped fiber lasers.

Chalcogenide glasses are a broad class of increasingly important technological materials used in phase-change memories, solar cells, sensors and non-linear optical devices. They almost invariably display p-type electronic conductivity, and are known to remain p-type when melted with common donor atoms. The ability to reverse the carrier type in these glasses would enable electronic devices to be integrated with other chalcogenide-glass-based devices and may enable the fabrication of LEDs and laser diodes that emit at novel wavelengths. Bi and Pb are the only known dopants to cause carrier-type reversal (CTR) in chalcogenide glasses by melt doping, mainly in germanium chalcogenides. The origin of this carrier-type reversal is also disputed. Phillips proposed a model for the microscopic structure of Bi-modified Ge_xB_{1-x} (B = S, Se or Te) glass as Bi_2B_3 clusters with a tetradymite-like structure embedded in a Ge_xB_{1-x} matrix [24]. This was based on differential thermal analysis (DTA) [25] and penetration probe [26] measurements which indicated a phase separation in the Bi-modified glasses. A.C. measurements indicate that these clusters may have n-type defects situated at excess S^{-} atoms on cluster surfaces; these defects may be taking part in a single-polaron hopping process [27]. However, on the basis of EXAFS measurements, Elliott *et al* argued that Bi is only

3-fold coordinated, and that the glasses were homogeneous without Bi_2S_3 clusters [28], and that the mechanism of CTR is due to the presence of charged Bi atoms which suppress the concentration of positively charged chalcogen defects at the expense of negatively charged defects. In 1989, a p-n junction based on the Ge-Se-Bi glass system was fabricated [29]. However, since this time there have not been significant strides in increasing the performance of these p-n junctions, which may be related to the lack of understanding of the physical process that underlies carrier-type reversal in these glasses.

Conventionally, Bi and Pb dopants are introduced into the glass melts ('melt-doping'). We define melt-doping as an equilibrium doping method because the dopants are able to react with the glass material, above the glass-transition temperature, T_g, for sufficient time for the dopants to achieve their lowest energy bonding configuration. We define non-equilibrium doping as the inclusion of a dopant into the glass matrix below T_g. Ion implantation is a precise, non-equilibrium doping technique which is essential to the fabrication of most modern integrated circuits (ICs). It is relevant to Bi-doped glasses because it may allow control over which Bi centers are present in the glass. It is also relevant for the development of high-performance electronic devices based on Bi-doped glasses because it is the most precise doping technique in use today, and it may be possible to reverse the carrier type of chalcogenide glasses by impurity doping under non-equilibrium conditions [30], as has been shown for Cd, Al, Zn and Mg (non-equilibrium) diffusion-doped $As_2Se_2Te_1$ glass [31-33]. In this work, we report, PL from Bi-implanted glasses and crystals. The PL spectra are different to those from similar materials that are melt doped with Bi. We also report PL from Bi doped chalcogenide glasses which have compositions very close to those in which carrier-type reversal has been reported, and suggest that these phenomena are produced by the same, or a similar, active center. If our hypothesis is correct, it may assist in hastening the elucidation of the origin of these phenomena.

2. Experimental

2.1 Sample preparation

A gallium lanthanum sulphur oxide (GLSO) sputtering target was prepared by mixing 70% gallium sulphide, and 30% lanthanum oxide in a dry-nitrogen purged glove box. The raw materials were melted for 24 hours in dry argon, in 2 inch diameter vitreous carbon crucibles, annealed at the glass-transition temperature and then sliced to form a 3mm thick sputter target. We sputtered 100 nm thick films of GLSO onto 1μm thick thermally oxidized SiO_2 on Si substrates. The RF sputtering power was 60W, with an Ar flow of 15 SCCM. Details of the fabrication of bulk Bi-doped GLSO [12], SiAlLiO [34] and can be found elsewhere. Fused silica glass, Schott NPSK53 phosphate glass, crystalline CaF_2 and BaF_2 polished bulk samples were purchased commercially. Bismuth ions were implanted using a Danfysik ion implanter at an energy of 190 keV. During implantation, the samples were mounted on a carousel holder held at ambient temperature, and the beam current was kept below 1 $\mu A/cm^2$ to avoid beam heating of the targets.

2.2 Sample characterization

PL spectra of bulk samples were obtained by exciting with a 808 nm laser diode, or 514 nm Ar- ion laser. The emission was dispersed by a Jasco CT-25C monochromator which used a 600 or 1200 lines/mm grating. The slit width was ~2.5 mm, which corresponded to a resolution of ~10 nm. The stray excitation light was blocked with appropriate long-pass filters. Detection was realized with a Hamamatsu H9170 NIR photomultiplier tube (PMT), Newport Si, or InGaS detectors, coupled with standard phase-sensitive detection. All spectral measurements were corrected for the wavelength-dependent response of the measurement system by calculating a correction spectrum (C(λ)), with $C(\lambda)=I_{cal}(\lambda)/I_{meas}(\lambda)$, where $I_{meas}(\lambda)$ is the luminescence spectrum of an Ushio calibrated white-light source measured by the detection system and $I_{cal}(\lambda)$ is the luminescence spectrum of the calibrated white-light source supplied by the manufacturer. Due to their weak emission, PL spectra of implanted samples were taken on a Renishaw 2000 microRaman system incorporating a Si CCD detector array, with a detection range of 400 – 1100 nm, and 514 or 782 nm excitation laser lines. A 50x microscope objective was used to focus the excitation onto the implanted sample surface. Several spectra were taken at different positions on the sample and then averaged. It was found that the variation in PL intensity between different positions on the same sample was less than 5%. This technique can therefore be used to compare the relative PL intensity between different implants. We also measured the PL from unimplanted samples to account for any PL that could be coming from the unimplanted film or substrate. These spectra were then subtracted from the PL spectra of the implanted samples. The PL intensity of unimplanted samples was less than around 5% of that of the implanted samples in the thin-film samples, and less than 25% in the bulk samples. Spectra were corrected by measuring the broadband PL of a Bi-doped glass with a known spectral luminance. Ripples in some of the PL spectra measured on the Raman system are an artifact caused by the various filters. Differential thermal analysis (DTA) measurements were taken using a Rigaku Thermo Plus TG-DTA. Rutherford back-scattering (RBS) measurements were made on a 2MV Tandetron accelerator using 2 MeV He beams.

3. Results and discussion

3.1 Melt-doped oxides and chalcogenides

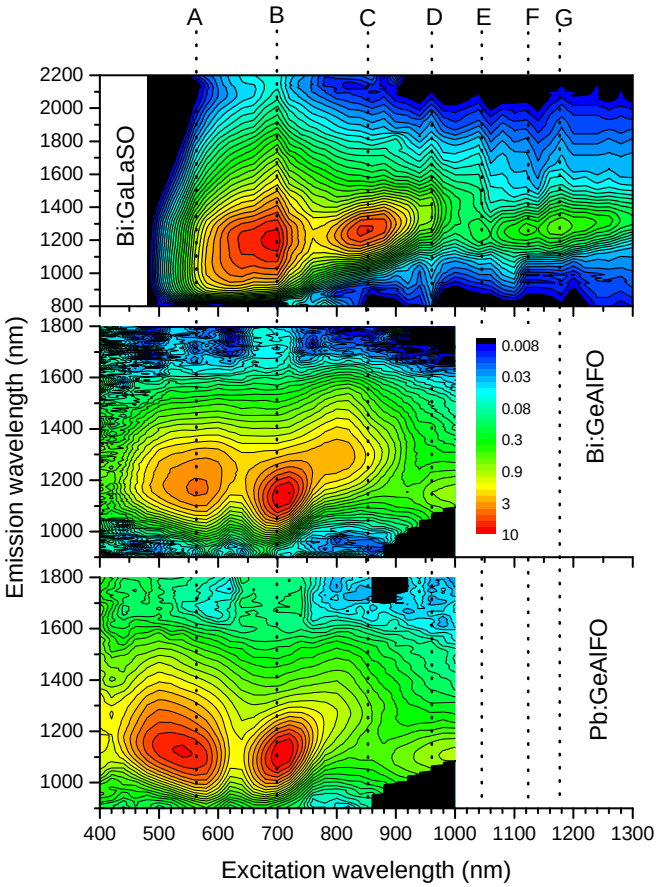

Figure 1 Contour plots of PL emission from Bi-doped GLSO, after [12], and Bi- and Pb-doped germanate bulk glasses, after [15]. The intensity is plotted on a log scale.

Figure 1 shows contour plots, which are comprised of a series of PL spectra over a range of excitation wavelengths, of bulk melt-doped glasses: $Ga_{28}La_{12}S_{56}O_4Bi_{0.4}$ (Bi:GLSO), after [12], $Ge_{28}O_{56}F_{11}A1_4Bi_{0.6}$ (Bi:GeAlFO), and $Ge_{28}O_{56}F_{12}A14Pb_{0.3}$ (Pb:GeAlFO), after [15]. These contour plots can be used to determine the position of absorption and PL bands. Strong absorption/PL bands show up clearly as islands on the contour plot; weaker absorption/PL bands show up as kinks and bends in the contour lines. In Fig 1, we identified seven absorption/PL bands in Bi:GLSO, marked A-G. Band A is rather indistinct in Bi:GLSO, which may be caused by the strong band-edge absorption of GLSO in this region. However, there is a clear change in direction of the contour lines at 565 nm, indicating the presence of an absorption/PL band, which lines up almost exactly with the strong band in Bi:GeAlFO. Band D is evident only as a kink in contour lines in Bi:GeAlFO at 960 nm, and is not evident in Pb:GeAlFO. Much of band E is missing in the germanate glasses; however, it is not much greater than 1000 nm. We find that the positions of 5 absorption/PL bands are approximately the same in Bi- and Pb-doped germanate glass and Bi-doped chalcogenide glass, indicating that they are related to essentially the same optical center. Similar absorption and emission properties were also observed in Bi- and Pb-doped calcium phosphate and sodium silicate glasses [35]. The origin of this similarity is intriguing. Similar NIR PL bands have been reported from Bi, Pb, Sb and Sn doped germanate glasses [15], and since spin-orbit constants are so dissimilar for these elements, it has been argued that the NIR PL did not originate from dopant centers. We suggest, however, that there may be similarities in the energy level structure of complex clusters of these elements, which could produce similar NIR PL bands.

3.3 Ion-implanted optical materials

Figure 2 shows the PL spectra of Bi-implanted GLSO films along with bulk phosphate and silica glass, and crystalline CaF_2 and BaF_2, excited at 782 nm. Damage related optical centers are known to produce PL, however, when implanted

with other species such as Ag and V, no PL was observed. This indicates that the observed PL is related to a Bi center, rather than damage caused by the implantation. The Bi implanted samples all display a PL peak at 800 to 880 nm. Phosphate glass has a PL peak at 800 nm, which is very close to the excitation wavelength. GLSO and silica both have a main PL peak at 820 nm, with GLSO having a shoulder at 920 nm. Crystalline BaF_2 has a peak at 845 nm with evidence of a shoulder at 960 nm. Crystalline CaF_2 has a single broad peak at 880 nm. When melt doped with Bi in bulk and excited at 800 nm, phosphate glass had broad PL peaking at 1300 nm [36], silica glass at 1250 nm [37] and crystalline BaF_2 at 1100 nm [38]. This result indicates that ion implantation is able to generate Bi centers which are not present in samples whose dopants are introduced during melting. This is important for the application of Bi implantation as a non-equilibrium doping technique because it indicates that the Bi does not achieve its lowest energy bonding configuration as we expect it to during melt doping. The intensity of the PL varied over two orders of magnitude between the phosphate and silica glass host.

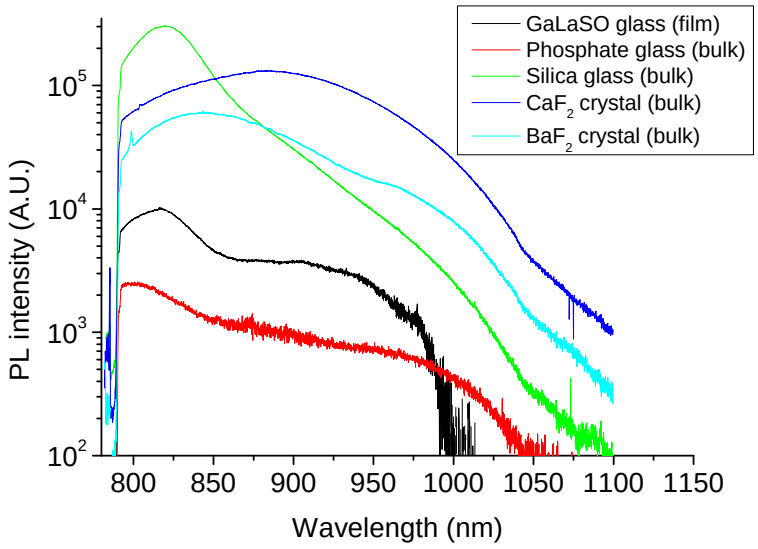

Figure 2 PL spectra of Bi -implanted GLSO thin film, bulk phosphate and silica glass, and crystalline CaF_2 and BaF_2, at dose of $3x10^{15}$ ions/cm^2. Excitation was at 782 nm.

Figure 3 shows the PL spectra of Bi-implanted GLSO thin films at various doses, along with bulk Bi-melt-doped GLSO and Li_2O-Al_2O_3-SiO_2 (LiAlSiO) glass, excited at 514 nm. Bulk Bi:GLSO exhibits a PL peak at 950 nm. However, the $1x10^{14}$ ions/cm^2 Bi-implanted GLSO has a characteristic red PL band, peaking at 700 nm, which is commonly observed in Bi-doped oxide glasses under green excitation [39]. The spectrum of the Bi: LiAlSiO glass in Figure 3 also has a 700 nm PL band, which is very similar to that of the $1x10^{14}$ ions/cm^2 Bi-implanted GLSO. Comparing the $1x10^{15}$ ions/cm^2 Bi implant to bulk Bi:GLSO (which have very similar compositions) indicates that the $1x10^{15}$ ions/cm^2 Bi implant has the 700 nm PL band associated with oxide glasses, and the 950 nm PL band observed in bulk Bi:GLSO, in equal intensities. If we extend our model of oxide glasses, in which red and NIR PL result from Bi^{2+} and Bi_n clusters, respectively,[40] to Bi:GLSO, then implanted Bi is more likely to be incorporated as Bi^{2+} than melt-doped Bi. The 700 nm PL band remains approximately constant for $1x10^{14}$ and $1x10^{15}$ ions/cm^2 Bi implants, which is similar to the effect discussed earlier for Bi:SiMgAlO [39]. For the $1x10^{16}$ ions/cm^2 Bi implant, the 700 nm PL band becomes stronger. We were unable to detect any NIR PL from the implanted samples using the standard measurement system that we used for our bulk samples.

During ion implantation, accelerated ions are decelerated by collisions with the nuclei, and electronic clouds, of atoms in the target. After a series of collisions, the implanted ion comes to rest. These collisions result in the displacement of individual atoms, which causes damage to the atomic structure of the target. In silicon IC manufacture, this damage is usually relieved by subsequent annealing above the crystallization temperature. This annealing activates the dopant by allowing them to move from an interstitial site to a lattice site. Similarly to ion-implanted Si, we expect that ions implanted into chalcogenide glasses will initially enter interstitial sites. XPS and NEXAFS measurements of N_2-implanted and nitrogen-codeposited $Ge_2Sb_2Te_5$ amorphous chalcogenide films indicated that implanted N tended to accumulate in interstitial sites compared to codeposited N_2 [41]. This indicates that Bi^{2+} associated with Bi-implanted GLSO may be interstitial.

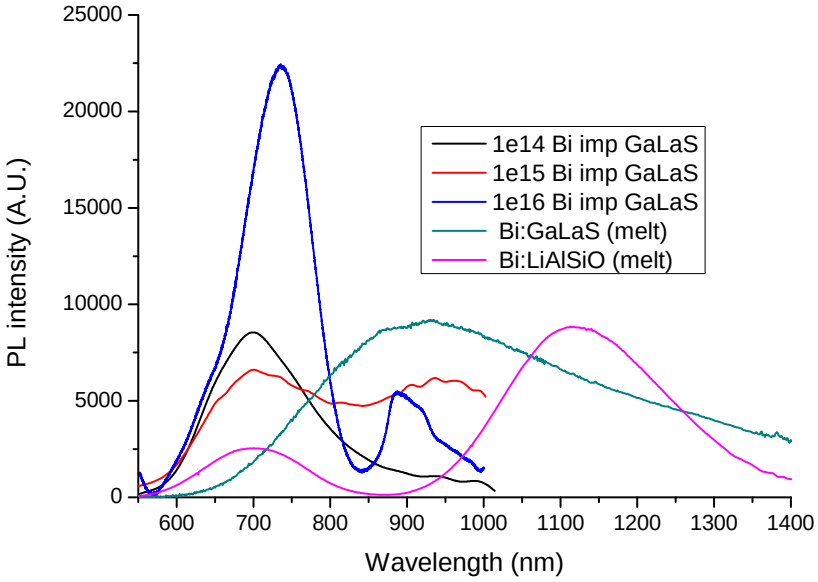

Figure 3 PL spectra of Bi- and Pb-implanted GLSO films at various doses, and bulk Bi-doped GLSO and LiAlSiO glass, excited at 514 nm. The PL intensities of the implanted films are plotted relative to each other, the bulk samples are not.

Bi- and Pb-doped chalcogenides are the only melt-doped chalcogenide glasses in which carrier-type reversal has been observed. Investigators of this phenomenon have usually fabricated a series of Bi- or Pb-doped chalcogenide glasses in which the doping content is increased, and measured the thermopower as a function of dopant content. In Bi-doped GeGaS glass, the addition of Bi caused a red-shift in the absorption edge, rather than the appearance of characteristic Bi absorption bands observed in oxide glasses [11]. In fact, the addition of just 0.15 at.% Bi caused a red-shift in the band edge of around 100 nm. A similar red-shift is observed when Bi is added to GeB (B=S, Se, Te) glasses in which CTR is observed [42], and this red-shift is associated with the CTR. Figure 4(a) shows characteristic Bi-related PL from a Bi-doped GeGaS glass ($Ge_{23}Ga_{12}S_{64}Bi_1$) [11]; at lower Bi concentrations, the PL peak is very similar to a Bi-doped germanate glass. With increasing Bi concentration, the PL becomes significantly weaker and shifts to longer wavelengths. This is probably related to the large red-shift in band edge caused by the addition of Bi. The composition of this glass is very similar to those of glasses in which CTR has been observed ($Ge_{20}Sb_{11}S_{65}Bi_4$ and $Ge_{20}S_{73}Bi_7$), as shown in Figure 4(b). It is therefore reasonable to assume that similar Bi centers are generated in glasses displaying CTR and PL. Since PL in Bi-doped glasses is widely thought to originate from multiple Bi centers, it is likely that one or more of these centers causes the CTR. The observation of NIR PL would suggest this center is Bi clusters [40].

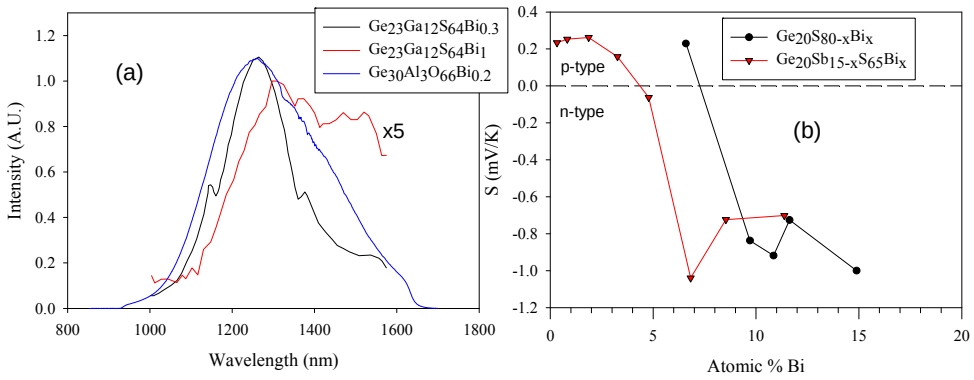

Figure 4 (a) PL spectra of Bi-doped GeGaS, after [11], and Bi-doped germanate glass, with 808 nm excitation. (b) Thermopower as a function of Bi content in GeS glass, after [26], and in GeSbS glass, after [43] .

4. Conclusions

Comparing contour plots of PL spectra at various excitation wavelengths of Bi-doped chalcogenide, Bi-doped germanate and Pb-doped germanate glasses, indicates that five absorption/PL bands are in approximately the same position. This suggests that very similar active centers are present in Bi- and Pb-doped oxide and chalcogenide glasses. When excited at 782 nm, Bi-implanted GaLaSO thin films along with bulk phosphate and silica glass, and BaF_2 crystal all display characteristic narrow PL peaking between 800 and 880 nm, whereas when melt-doped these materials display broad PL peaking between 1100 and 1300 nm. When excited at 514 nm, Bi-implanted GaLaSO thin films display a PL band at 700 nm, which is not present in a Bi melt-doped chalcogenide glass having a similar composition to the implanted glass. This indicates that new Bi centers are formed through implantation, which are absent in the melt-doped glasses. This has important implications for Bi-doped glass lasers, in which the control of Bi centers is critical for improving performance. We highlight NIR PL bands in $Ge_{23}Ga_{12}S_{64}Bi_1$ glass which has a very similar composition to those in which carrier-type reversal has been observed. This indicates that Bi-related PL and carrier-type reversal may be caused by the same Bi centers, which we suggest are interstitial Bi^{2+} and Bi clusters.

Acknowledgments
This work was supported by the UK EPSRC grants EP/I018414/1, EP/I019065/1 and EP/I018050/1.

REFERENCES

1. G. W. Chi, D. C. Zhou, Z. G. Song, and J. B. Qiu, "Effect of optical basicity on broadband infrared fluorescence in bismuth-doped alkali metal germanate glasses," Opt. Mater. **31**, 945-948 (2009).
2. A. N. Romanov, Z. T. Fattakhova, A. A. Veber, O. V. Usovich, E. V. Haula, V. N. Korchak, V. B. Tsvetkov, L. A. Trusov, P. E. Kazin, and V. B. Sulimov, "On the origin of near-IR luminescence in Bi-doped materials (II). Subvalent monocation Bi^+ and cluster Bi_5^{3+} luminescence in $AlCl_3/ZnCl_2/BiCl_3$ chloride glass," Opt. Express **20**, 7212-7220 (2012).
3. M. Peng, D. Chen, J. Qiu, X. Jiang, and C. Zhu, "Bismuth-doped zinc aluminosilicate glasses and glass-ceramics with ultra-broadband infrared luminescence," Opt. Mater. **29**, 556-561 (2007).
4. Y. Arai, T. Suzuki, Y. Ohishi, S. Morimoto, and S. Khonthon, "Ultrabroadband near-infrared emission from a colorless bismuth-doped glass," Appl. Phys. Lett. **90**, 261110 (2007).
5. M. Peng, B. Wu, N. Da, C. Wang, D. Chen, C. Zhu, and J. Qiu, "Bismuth-activated luminescent materials for broadband optical amplifier in WDM system," J. Non-Cryst. Solids **354**, 1221-1225 (2008).
6. J. Ren, J. Qiu, B. Wu, and D. Chen, "Ultrabroad infrared luminescence from Bi-doped alkaline earth metal germanate glasses," J. Mater. Res. **22**, 1574-1577 (2007).
7. M. Peng, J. Qiu, D. Chen, X. Meng, I. Yang, X. Jiang, and C. Zhu, "Bismuth and aluminium codoped germanium oxide glasses for super-broadband optical amplification," Opt. Lett. **29**, 1998-2000 (2004).
8. M. Peng, J. Qiu, D. Chen, X. Meng, and C. Zhu, "Superbroadband 1310 nm emission from bismuth and tantalum codoped germanium oxide glasses," Opt. Lett. **30**, 2433-2435 (2005).
9. X. G. Meng, J. R. Qiu, M. Y. Peng, D. P. Chen, Q. Z. Zhao, X. W. Jiang, and C. S. Zhu, "Near infrared broadband emission of bismuth-doped aluminophosphate glass," Opt. Express **13**, 1628-1634 (2005).
10. X. G. Meng, J. R. Qiu, M. Y. Peng, D. P. Chen, Q. Z. Zhao, X. W. Jiang, and C. S. Zhu, "Infrared broadband emission of bismuth-doped barium-aluminum-borate glasses," Opt. Express **13**, 1635-1642 (2005).
11. G. P. Dong, X. D. Xiao, J. J. Ren, J. Ruan, X. F. Liu, J. R. Qiu, C. G. Lin, H. Z. Tao, and X. J. Zhao, "Broadband infrared luminescence from bismuth-doped GeS_2-Ga_2S_3 chalcogenide glasses," Chin. Phys. Lett. **25**, 1891-1894 (2008).
12. M. A. Hughes, T. Akada, T. Suzuki, Y. Ohishi, and D. W. Hewak, "Ultrabroad emission from a bismuth doped chalcogenide glass," Opt. Express **17**, 19345-19355 (2009).
13. Y. Fujimoto and M. Nakatsuka, "Infrared Luminescence from Bismuth-Doped Silica Glass," Jpn. J. Appl. Phys. Part 2 Lett. **40**, L279-L281 (2001).
14. X. Wang and H. Xia, "Infrared superbroadband emission of Bi ion doped germanium-aluminum-sodium glass," Opt. Commun. **268**, 75-78 (2006).
15. M. Y. Sharonov, A. B. Bykov, V. Petricevic, and R. R. Alfano, "Spectroscopic study of optical centers formed in Bi-, Pb-, Sb-, Sn-, Te-, and In-doped germanate glasses," Opt. Lett. **33**, 2131-2133 (2008).
16. S. Khonthon, S. Morimoto, Y. Arai, and Y. Ohishi, "Luminescence Characteristics of Te- and Bi-Doped Glasses and Glass-Ceramics," J. Ceram. Soc. Jpn. **115**, 259-263 (2007).
17. V. O. Sokolov, V. G. Plotnichenko, and E. M. Dianov, "Origin of broadband near-infrared luminescence in bismuth-doped glasses," Opt. Lett. **33**, 1488-1490 (2008).

18. I. A. Bufetov and E. M. Dianov, "Bi-doped fiber lasers," Laser Phys. Lett. **6**, 487-504 (2009).
19. S. V. Firstov, A. V. Shubin, V. F. Khopin, M. A. Mel'kumov, I. A. Bufetov, O. I. Medvedkov, A. N. Guryanov, and E. M. Dianov, "Bismuth-doped germanosilicate fibre laser with 20-W output power at 1460 nm," Quantum Electron. **41**, 581 (2011).
20. V. V. Dvoyrin, V. M. Mashinsky, and E. M. Dianov, "Efficient Bismuth-Doped Fiber Lasers," IEEE J. Quantum Elect. **44**, 834-840 (2008).
21. S. Kivisto, J. Puustinen, M. Guina, O. G. Okhotnikov, and E. M. Dianov, "Tunable modelocked bismuth-doped soliton fibre laser," Electron. Lett. **44**, 1456-1458 (2008).
22. A. B. Rulkov, A. A. Ferin, S. V. Popov, J. R. Taylor, I. Razdobreev, L. Bigot, and G. Bouwmans, "Narrow-line, 1178nm CW bismuth-doped fiber laser with 6.4W output for direct frequency doubling," Opt. Express **15**, 5473-5476 (2007).
23. S. Yoo, M. P. Kalita, J. Sahu, J. Nilsson, and D. Payne, "Bismuth-doped fiber laser at 1.16 mm," in *Lasers and Electro-Optics, Conference on Quantum Electronics and Laser Science. CLEO/QELS*, 2008), 1-2.
24. J. C. Phillips, "Constraint theory and carrier-type reversal in Bi-Ge chalcogenide alloy glasses," Phys. Rev. B **36**, 4265-4270 (1987).
25. K. L. Bhatia, D. P. Gosain, G. Parthasarathy, and E. S. R. Gopal, "On the structural features of doped amorphous chalcogenide semiconductors," J. Non-Cryst. Solids **86**, 65-71 (1986).
26. L. Tichý, H. Tichá, A. Třiska, and P. Nagels, "Is the n-type conductivity in some Bi-doped chalcogenide glasses controlled by percolation?," Solid State Commun. **53**, 399-402 (1985).
27. V. K. Bhatnagar and K. L. Bhatia, "Frequency dependent electrical transport in bismuth-modified amorphous germanium sulfide semiconductors," J. Non-Cryst. Solids **119**, 214-231 (1990).
28. S. R. Elliott and A. T. Steel, "Mechanism for Doping in Bi Chalcogenide Glasses," Phys. Rev. Lett. **57**, 1316-1319 (1986).
29. P. Kounavis, E. Mytilineou, and M. Roilos, "p-n junctions from sputtered $Ge_{25}Se_{75-x}Bi_x$ films," J. App. Phys. **66**, 708-710 (1989).
30. H. Fritzsche and M. Kastner, "The effect of charged additives on the carrier concentrations in lone-pair semiconductors," Philos. Mag. B **37**, 285-292 (1978).
31. S. Okano, H. Yamakawa, M. Suzuki, and A. Hiraki, "Fabrication of Chalcogenide Amorphous Semiconductor Diodes Using Low Temperature Thermal Diffusion Techniques," Jpn. J. Appl. Phys. **26**, 1102-1106 (1987).
32. S. Okano, M. Suzuki, T. Imura, and A. Hiraki, "Chalcogenide amorphous-semiconductor diodes," Jpn. J. Appl. Phys. Part 2 Lett. **24**, L445-L448 (1985).
33. S. Okano and M. Suzuki, "Electrical contact properties of metal-chalcogenide amorphous-semiconductor systems," Jpn. J. Appl. Phys. **20**, 1635-1640 (1981).
34. T. Suzuki and Y. Ohishi, "Ultrabroadband near-infrared emission from Bi-doped Li_2O-Al_2O_3-SiO_2 glass," Appl. Phys. Lett. **88**, 191912 (2006).
35. S. Parke and R. S. Webb, "The optical properties of thallium, lead and bismuth in oxide glasses," J. Phys. Chem. Solids **34**, 85 (1973).
36. X. G. Meng, J. R. Qiu, M. Y. Peng, D. P. Chen, Q. Z. Zhao, X. W. Jiang, and C. S. Zhu, "Near infrared broadband emission of bismuth-doped aluminophosphate glass," Opt. Express **13**, 1628-1634 (2005).
37. Y. Fujimoto and M. Nakatsuka, "Infrared Luminescence from Bismuth-Doped Silica Glass," Jpn. J. Appl. Phys., Part 2 **40**, L279-L281 (2001).
38. J. Ruan, L. B. Su, J. R. Qiu, D. P. Chen, and J. Xu, "Bi-doped BaF_2 crystal for broadband near-infrared light source," Opt. Express **17**, 5163-5169 (2009).
39. B. I. Denker, B. I. Galagan, V. V. Osiko, I. L. Shulman, S. E. Sverchkov, and E. M. Dianov, "Factors affecting the formation of near infrared-emitting optical centers in Bi-doped glasses," Appl. Phys. B-Lasers Opt. **98**, 455-458 (2010).
40. M. A. Hughes, R. M. Gwilliam, K. Homewood, B. Gholipour, D. W. Hewak, T.-H. Lee, S. R. Elliott, T. Suzuki, Y. Ohishi, T. Kohoutek, and R. J. Curry, "On the analogy between photoluminescence and carrier-type reversal in Bi- and Pb-doped glasses " Opt. Express **21**, 8101-8115 (2013).
41. Y. Kim, J. H. Baeck, M.-H. Cho, E. J. Jeong, and D.-H. Ko, "Effects of N^{2+} ion implantation on phase transition in $Ge_2Sb_2Te_5$ films," J. App. Phys. **100**, 083502 (2006).
42. N. Tohge, T. Minami, Y. Yamamoto, and M. Tanaka, "Electrical and optical properties of n-type semiconducting chalcogenide glasses in the system Ge-Bi-Se," J. App. Phys. **51**, 1048-1053 (1980).
43. J. Málek, J. Klikorka, L. Beneš, L. Tichý, and A. Tříska, "Electrical and optical properties of $Ge_{20}Sb_{15-x}Bi_xBi_{65}$ glasses," J. Mater. Sci. **21**, 488-492 (1986).